the plant journal

SEB Society for Experimental Biology

The Plant Journal (2015) **84,** 847–859 doi: 10.1111/tpj.13064

Arabidopsis thaliana isoprenyl diphosphate synthases produce the C_{25} intermediate geranylfarnesyl diphosphate

Raimund Nagel[1,†], Carolin Bernholz[2], Eva Vranová[3], Ján Košuth[3], Nick Bergau[2], Steve Ludwig[4], Ludger Wessjohann[4], Jonathan Gershenzon[1], Alain Tissier[2] and Axel Schmidt[1,*]

[1]*Department of Biochemistry, Max Planck Institute for Chemical Ecology, Beutenberg Campus, Hans Knoell Straße 8, D–07745 Jena, Germany,*

[2]*Department of Cell and Metabolic Biology, Leibniz Institute of Plant Biochemistry, Weinberg 3, D–06120 Halle (Saale), Germany,*

[3]*Institute of Biology and Ecology, Pavol Jozef Šafárik University Košice, Mánesova 23, 04154 Košice, Slovakia, and*

[4]*Department of Bioorganic Chemistry, Leibniz Institute of Plant Biochemistry, Weinberg 3, D–06120 Halle (Saale), Germany*

Received 15 June 2015; revised 11 September 2015; accepted 21 October 2015; published online 27 October 2015.

*For correspondence (e-mail aschmidt@ice.mpg.de).

†Present address: Roy J. Carver, Department of Biochemistry, Biophysics & Molecular Biology, Iowa State University, 4216 Molecular Biology Building, Ames, IA 50011, USA.

SUMMARY

Isoprenyl diphosphate synthases (IDSs) catalyze some of the most basic steps in terpene biosynthesis by producing the prenyl diphosphate precursors of each of the various terpenoid classes. Most plants investigated have distinct enzymes that produce the short-chain all-*trans* (*E*) prenyl diphosphates geranyl diphosphate (GDP, C_{10}), farnesyl diphosphate (FDP, C_{15}) or geranylgeranyl diphosphate (GGDP, C_{20}). In the genome of *Arabidopsis thaliana*, 15 *trans*-product-forming IDSs are present. Ten of these have recently been shown to produce GGDP by genetic complementation of a carotenoid pathway engineered into *Escherichia coli*. When verifying the product pattern of IDSs producing GGDP by a new LC-MS/MS procedure, we found that five of these IDSs produce geranylfarnesyl diphosphate (GFDP, C_{25}) instead of GGDP as their major product in enzyme assays performed *in vitro*. Over-expression of one of the GFDP synthases in *A. thaliana* confirmed the production of GFDP *in vivo*. Enzyme assays with *A. thaliana* protein extracts from roots but not other organs showed formation of GFDP. Furthermore, GFDP itself was detected in root extracts. Subcellular localization studies in leaves indicated that four of the GFDP synthases were targeted to the plastoglobules of the chloroplast and one was targeted to the mitochondria. Sequence comparison and mutational studies showed that the size of the R group of the 5th amino acid residue N-terminal to the first aspartate-rich motif is responsible for C_{25} versus C_{20} product formation, with smaller R groups (Ala and Ser) resulting in GGDP (C_{20}) as a product and a larger R group (Met) resulting in GFDP (C_{25}).

Keywords: sesterterpenes, terpenes, geranylfarnesyl diphosphate, geranylgeranyl diphosphate, isoprenyl diphosphate synthase, prenyltransferase, *Arabidopsis thaliana*.

INTRODUCTION

Despite the enormous structural diversity of over 60 000 known terpene natural products (Koksal *et al.*, 2011), the initial steps of terpene biosynthesis are highly conserved. The basic C_5 building blocks of all terpenes, isopentenyl diphosphate (IDP) and dimethylallyl diphosphate (DMADP), are similar for all terpenes, and are synthesized by two pathways: the mevalonate and the methylerythritol phosphate pathways (Arigoni *et al.*, 1997; Rodríguez-Concepción, 2006; Vranová *et al.*, 2013). For biosynthesis of all terpenes larger than C_5, isoprenyl diphosphate synthases (IDSs) are required to condense the basic C_5 building blocks, forming C_{10}, C_{15}, C_{20} and larger prenyl diphosphates. The IDS products then act as substrates for terpene synthases that give rise to the enormous variety of terpene skeletons produced (Tholl, 2006; Degenhardt *et al.*, 2009).

By controlling the size of the prenyl diphosphate intermediates formed, IDSs control the major groups of terpenes formed. Short-chain IDSs typically catalyze the sequential head-to-tail condensation of IDP with an allylic

substrate, usually either DMADP (C_5), geranyl diphosphate (GDP, C_{10}) or farnesyl diphosphate (FDP, C_{15}). Depending on the geometry of the double bond in the product formed, IDSs are classified as either *cis*- or *trans*-IDSs (Liang *et al.*, 2002). Although these two types perform almost the same reactions, they are evolutionarily and structurally distinct from each other. The catalytic activity of *trans*-IDSs depends on the first and second aspartate-rich motifs (FARM and SARM, respectively). The FARM motif has either the sequence DDxxD or DDxxxxD, whereas the SARM motif is always DDxxD. Both motifs bind three Mg^{2+} ions, which in turn collectively bind the homoallylic substrate IDP, and one of the allylic substrates (DMADP, GDP or FDP), and thereby coordinate formation of longer products (Aaron and Christianson, 2010). The product specificity of short-chain *trans*-IDSs is to a large extent regulated by the identity of the amino acids on the N–terminal side of the FARM. The so-called 'molecular ruler theory' hypothesizes that the size of the side chain of these amino acids limits the dimensions of the active-site pocket (Wang and Ohnuma, 2000; Liang *et al.*, 2002; Schmidt *et al.*, 2010).

The *cis*-IDSs generally produce longer prenyl diphosphates than *trans*-IDSs, with up to 5000 C_5 units in natural rubber. However, recently, a group of short-chain *cis*-IDSs was described in several tomato species (Sallaud *et al.*, 2009; Schilmiller *et al.*, 2009; Akhtar *et al.*, 2013), and a medium and long-chain *trans*-IDS that forms C_{25}–C_{45} products was reported in *Arabidopsis thaliana* (Hsieh *et al.*, 2011). Most *cis*- and *trans*-IDSs are homodimeric proteins, but heterodimeric IDSs have also been described, composed of a canonical IDS protein with two aspartate-rich motifs that produces GGDP by itself, plus a smaller IDS-like sequence that lacks one of the aspartate-rich motifs and is catalytically inactive by itself. These heterodimers produce shorter-chain products, either pure GDP or varying proportions of GDP and GGDP (Burke *et al.*, 2004; Tholl *et al.*, 2004; Wang and Dixon, 2009; Chang *et al.*, 2010).

In the genome of *Arabidopsis thaliana*, 15 short-chain *trans*-IDSs are present. One IDS that was originally shown to produce GDP (C_{10}) (Bouvier *et al.*, 2000) was more recently shown to produce C_{25}–C_{45} prenyl diphosphates instead (Hsieh *et al.*, 2011). Two other IDSs produce FDP (Closa *et al.*, 2010). Of the remaining 12 enzymes, ten have been shown to produce GGDP (C_{20}), most recently demonstrated by genetic complementation of a mutant carotenoid pathway engineered in *Escherichia coli* using *Erwinia uredovora* genes but lacking an active GGDP synthase (Zhu *et al.*, 1997a,b; Wang and Dixon, 2009; Beck *et al.*, 2013). Surprisingly, many of these GGDP synthases are expressed only in the roots (Beck *et al.*, 2013). None of these have been shown to form geranylfarnesyl diphosphate (GFDP, C_{25}), and no other short-chain plant IDS has yet been reported to form this product, although C_{25} terpenoids, known as sesterterpenoids, have occasionally been reported in plants. However, IDSs that principally form GFDP are known to exist in Archaea (Tachibana, 1994; Tachibana *et al.*, 2000; Ogawa *et al.*, 2010). Having developed a new LC-MS/MS-based analytical method for sensitive detection of IDS products (Nagel *et al.*, 2012), we re-investigated the catalytic activity of the *A. thaliana* GGDP synthases, and found surprisingly that some show geranylfarnesyl diphosphate (GFDP) synthase activity.

RESULTS

Arabidopsis thaliana IDSs form geranylfarnesyl diphosphate (GFDP) after expression in E. coli and A. thaliana

Arabidopsis thaliana GGDP synthase 1 (GGDPS1) has been described as an enzyme that produces geranylgeranyl diphosphate (GGDP, C_{20}) on the basis of a crude TLC-based assay (Okada *et al.*, 2000) and by genetic complementation of a mutation in carotenoid biosynthesis (Beck *et al.*, 2013). However, when we heterologously expressed the encoding gene in *E. coli* as a GST fusion construct, provided IDP and DMADP as substrates, and analyzed the enzyme product by LC-MS, a mixture of substances was detected. The most abundant product was the C_{25} compound geranylfarnesyl diphosphate (GFDP, 72% of the total), identified by comparison of its mass spectrum and retention time with those of an authentic standard, followed by GGDP (25%) and a trace of geranyl diphosphate (GDP, C_{10}, 2%) (Figure 1 and Table S1). As GGDP was not actually the major product of this enzyme, named as *At*GGDPS1, we subsequently refer to it and the other *At*GGDPS enzymes by the more general term isoprenyl diphosphate synthases (*At*IDSs) but retaining the enzyme number given previously (Tholl and Lee, 2011).

Comparison of the amino acid sequence of *At*IDS1 with those of other *At*IDSs showed an interesting polymorphism at position 175, five residues N–terminal to the first aspartate-rich motif (FARM), which has been shown to control product length. Position 175 is occupied by Ala in *At*IDS1 and Met or Ser in all other *At*IDS members (Figure 2). Upon heterologous expression, *At*IDS6, 7, 9 and 10 (all with Ser at position 175) gave GFDP as the major product (80–94% of the total), with only minor amounts of GDP or GGDP (Figure 3 and Table S1), while *At*IDS2 and 11 (Met at position 175) gave GGDP as the major product, with traces of GDP but no GFDP (Figure S1). *At*IDS5 was not cloned and tested, as it has been reported to have a frameshift mutation that introduces a stop codon early in the sequence (Beck *et al.*, 2013). *At*IDS3, *At*IDS4 and *At*IDS8 were also tested, but we did not observe any activity in the enzyme assays (Figure S1).

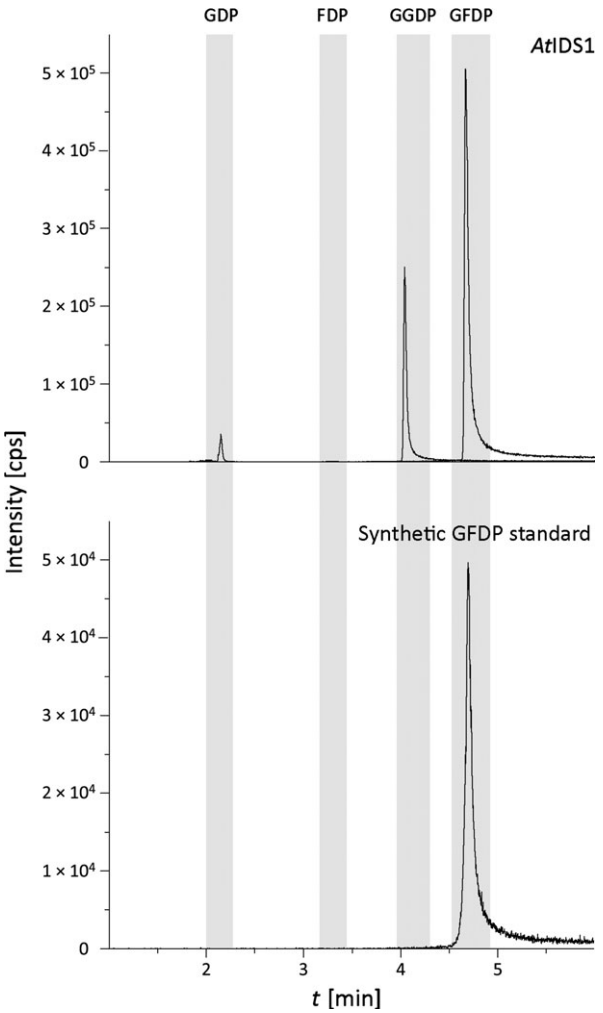

Figure 1. Heterologously expressed *A. thaliana* IDS1 has both geranylgeranyl diphosphate (GGDP, C_{20}) and geranylfarnesyl diphosphate (GFDP, C_{25}) synthase activity.
LC-MS/MS chromatograms are shown depicting the *in vitro* enzyme activity of *At*IDS1 (*At*1g49530) expressed in *E. coli* as a GST fusion construct and purified using a glutathione sepharose column. Also shown is the retention of a synthetic GFDP standard. Multiple reaction monitoring for GDP, FDP, GGDP and GFDP was performed in negative mode for $[M\text{-}H]^-$ and *m*/*z* 79 after fragmentation. The product distribution was calculated as: GFDP, 72.2%; GGDP, 25.1%; GDP, 2.4%; FDP, 0.3%. Three replicate assays were performed with very similar results.

To compare the *in vitro* reaction with various IDS substrates, one of the GFDP-synthesizing enzymes, *At*IDS9, was characterized in more detail by determining apparent K_m values for allylic substrates of varying lengths (from C_5 to C_{20}). The results summarized in Table 1 and Figure S2 indicate a higher affinity for the longer-chain substrates (GDP, FDP and GGDP) and for IDP than for DMADP.

To confirm our results regarding the product spectrum observed after expression in *E. coli*, we over-expressed *At*IDS9 (S175) and *At*IDS11 (M175) in *A. thaliana* Col-0 under the control of the CaMV 35S promoter. *At*IDS11 has been recently reported to be a GGDP synthase in *A. thaliana* that is required for the production of carotenoids, chlorophylls and all other primary plastid isoprenoids (Ruiz-Sola *et al.*, 2015). Analyses of IDS assays performed with protein extracts from leaves of these plants and leaves of wild-type controls showed that GFDP was only produced by plants over-expressing *At*IDS9. *At*IDS11 over-expression lines showed an increased GGDP activity in comparison to wild-type plants (Figure 4). Plants over-expressing *At*IDS9 also displayed a distinct growth phenotype in which young leaves had bleached patches that were not found on leaves of wild-type or *At*IDS11 over-expressing lines (Figure S3).

As further confirmation of GFDP versus GGDP product specificity *in vivo*, we over-expressed several IDS genes in the background of the loss-of-function *At*IDS11 mutant *ggpps11–4* (Ruiz-Sola *et al.*, 2015), which has an embryo-lethal phenotype due to the lack of GGDP. Expression of the genes encoding the GGDP-producing enzymes *At*IDS2 and 11 complemented this embryo-lethal phenotype, while those encoding the predominantly GFDP-producing enzymes *At*IDS6, 7, 9 and 10 (for which GGDP was present at <5% in the *in vitro* assay, Table S1) did not (Figure S4). These results further demonstrate that *At*IDS6–10 form little GGDP *in vivo* compared to *At*IDS2 and 11. On the other hand, *At*IDS1, a predominantly GFDP-producing enzyme that nonetheless forms a sizable amount of GGDP (25%, Table S1), did complement the embryo-lethal phenotype of *ggpps11–4* (Figure S4).

Arabidopsis GFDP synthases are localized in mitochondria and within the plastoglobules of plastids

Previous reports indicated that Arabidopsis IDSs localize to distinct subcellular compartments, including the mitochondria and the plastids (Okada *et al.*, 2000; Beck *et al.*, 2013). We considered it important to verify the locations of all the GFDP-forming enzymes (*At*IDS1, 6, 7, 9 and 10) in light of the newly described biochemical functions of these enzymes. To this end, C–terminal GFP fusions were generated and transiently expressed in *Nicotiana benthamiana*. The mitochondrial localization of *At*IDS1 was confirmed using a mitochondrial marker as described by Nelson *et al.* (2007) (Figure 5). In contrast, *At*IDS 6, 7, 9 and 10 all showed a plastidic localization, as previously shown by Beck *et al.* (2013), albeit with a conspicuous punctuate pattern. Similar within-plastid distributions have been observed for phytoene synthases from various organisms (Shumskaya *et al.*, 2012; Pasare *et al.*, 2013). To further investigate the identity of the spots found for *At*IDS 6, 7, 9 and 10, the Arabidopsis phytoene synthase (*At*PSY) was fused to the fluorescent marker mCherry in the C–terminal position. Merged images of the GFP and mCherry signals indicate a complete overlap, demonstrating co-localization of *At*PSY and *At*IDS 6, 7, 9 and 10.

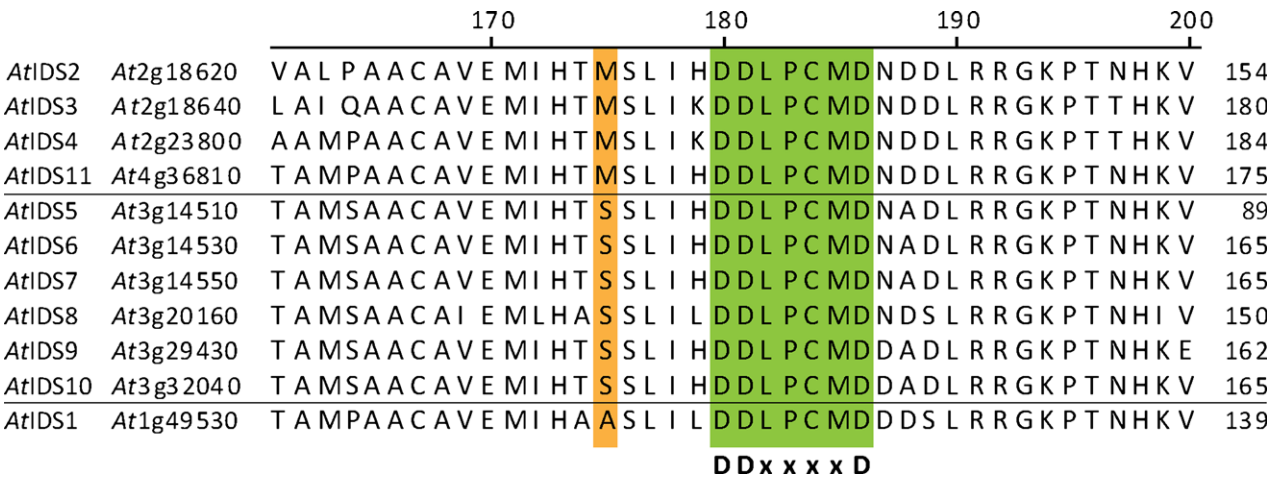

Figure 2. GFDP synthase activity is associated with specific amino acid residues.
Partial alignment of *A. thaliana* IDS is shown for the vicinity of the first arginine-rich motif (FARM, DDxxxxD, shown in green). Amino acids of all *A. thaliana* IDS previously reported to produce GGDP were aligned by ClustalW (www.clustal.org). The 5th position N-terminal to the FARM is highlighted in orange, and the sequences are sorted according to the amino acid present at this position.

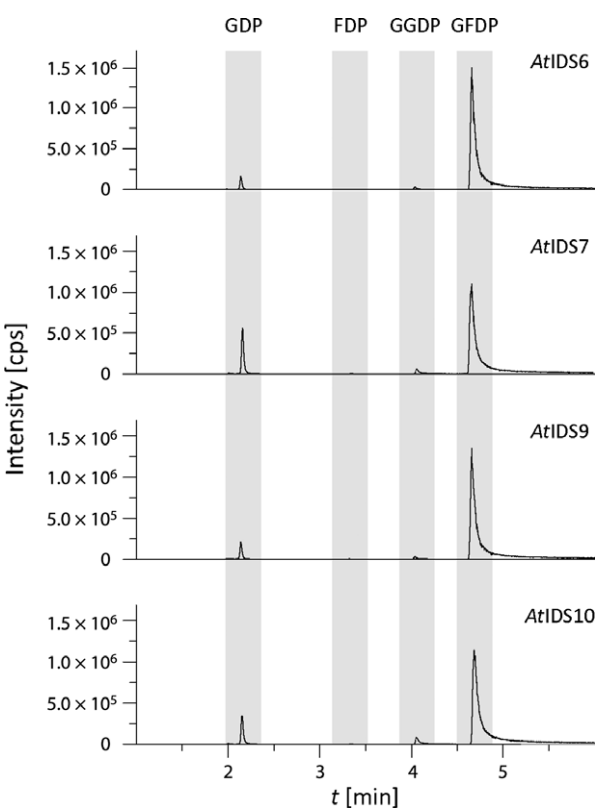

Figure 3. Heterologously expressed *A. thaliana* IDS6, IDS7, IDS9 and IDS10 principally have GFDP synthase activity.
LC-MS/MS chromatograms are presented to show the *in vitro* enzyme activities of *At*IDS6 (*At*3g14530), *At*IDS7 (*At*3g14550), *At*IDS9 (*At*3g29430) and *At*IDS10 (*At*3g32040) expressed in *E. coli* as a GST fusion construct and purified using a glutathione sepharose column. The product distributions were calculated as: 94% GFDP, 4% GDP and 2% GGDP for IDS6; 82% GFDP, 15% GDP and 4% GGDP for IDS7; 90% GFDP, 6% GDP and 4% GGDP for IDS9; 85% GFDP, 9% GDP and 6% GGDP for IDS10. At least three replicate assays were performed for each construct, with very similar results.

Table 1 Apparent *in vitro* K_m values of purified recombinant *Arabidopsis thaliana* IDS9

Varying substrate	Fixed substrate	K_m for the varying substrate (μM)
DMADP (0–100 μM)	IDP (100 μM)	47
GDP (0–50 μM)	IDP (100 μM)	17
FDP (0–50 μM)	IDP (100 μM)	12
GGDP (0–15 μM)	IDP (100 μM)	14
IDP (0–50 μM)	GGDP (50 μM)	11

Varying concentrations of DMADP, GDP, FDP and GGDP were incubated with 100 μM IDP, and varying concentrations of IDP were incubated with 50 μM GGDP. All assays contained 1 μg of purified recombinant protein at 20°C in a volume of 200 μl. Lineweaver–Burk plots are shown in Figure S2.

Furthermore, for IDS9, we found that 42 amino acids from the N–terminus were required for import into plastids, but were insufficient to confer the sub-organellar foci seen with the full-length protein (Figure S5), indicating that the signals for plastid import and sub-organellar distribution are distinct.

Change of a single amino acid residue near the first aspartate-rich motif leads to GFDP formation

To further explore the role of the amino acid residue at the 5th position N–terminal to the FARM in *At*IDS product specificity, we mutated the Ser residue of the GFDP-forming proteins *At*IDS6, 7, 9 and 10 into a Met. After expression, the mutated *At*IDS6, 7, 9 and 10 proteins (S175M) produced mainly GGDP and only small quantities of GFDP (Figure 6), showing the importance of Ser or Ala for GFDP formation.

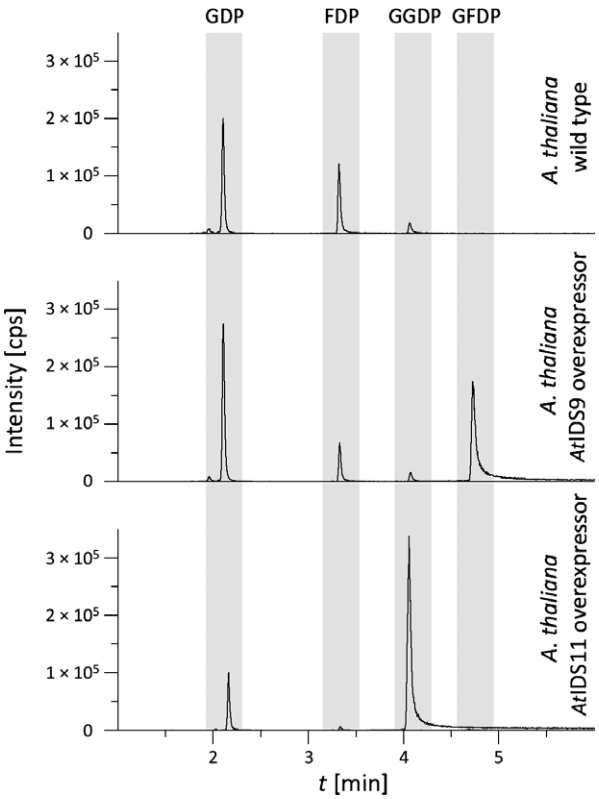

Figure 4. *At*IDS9 has GDFP activity upon expression in *A. thaliana*.
IDS activity was measured *in vitro* using total protein extracts prepared from leaves of *A. thaliana* over-expressing *At*IDS9 (S175) and AtIDS11 (M175) compared with wild-type plants. Representative LC-MS/MS chromatograms are shown. At least three replicate assays were performed for each genotype of each type, from at least five individual plants.

GFDP synthases are not part of a heterodimeric GGDP synthase

Arabidopsis thaliana possesses heterodimeric IDSs forming GDP or mixtures of GDP and GGDP. Combination of *At*IDS2 and 11, which were shown to be GGDP synthases when expressed alone, with a small subunit IDS was reported to give increased amounts of GDP as the product (Wang and Dixon, 2009). Therefore, we also analyzed the enzyme activity of one of the GFDP-forming IDSs, *At*IDS7, together with the small subunit, but did not observe a different product pattern between enzyme assays where *At*IDS7 was tested alone or in combination with the small subunit (Figure S6).

GFDP-forming activity and GFDP pools were found in A. thaliana root extracts

Previous reports suggested that GFDP-forming *At*IDS1, 6, 7, 9 and 10 were predominantly expressed in roots (Beck *et al.*, 2013; Coman *et al.*, 2014). To corroborate this, IDS assays were performed on a protein extract of *A. thaliana* Col–0 roots, and formation of GFDP was clearly detected (Figure 7), although the levels of GDP, FDP and GGDP formation were much higher than the formation of GFDP (Figure S7). However, GFDP formation was not seen in extracts of leaves and other organs (Figure 4). In addition, GFDP was also detected in methanol/water extracts of root tissue, as were GDP, FDP and GGDP (Figure 7 and Figure S7).

DISCUSSION

GFDP synthase activity has not been previously detected in plants

IDSs producing the C_{25} isoprenoid pathway intermediate GFDP have previously been reported from Archaea (Tachibana, 1994; Tachibana *et al.*, 2000; Ogawa *et al.*, 2010). Here we describe GFDP synthases from the plant *A. thaliana* that are 55–65% similar at the amino acid level to *A. thaliana* IDSs producing GGDP (Figure 8). Five enzymes (*At*IDS1, 6, 7, 9 and 10) were shown to form GFDP as the sole or dominant product. *At*IDS6 had previously been reported to produce a compound larger than GGDP, but this substance was not identified (Wang and Dixon, 2009). Other previous work had designated these *A. thaliana* enzymes as GGDP synthases. However, in some cases, activity was demonstrated by a genetic complementation assay for carotenoid biosynthesis using a set of genes from *E. uredovora* expressed in *E. coli* that lacked the necessary GGDP synthase (Zhu *et al.*, 1997b; Beck *et al.*, 2013). Our LC-MS/MS assay showed that GGDP was produced in at least trace amounts by these GFDP-forming enzymes, which explains their ability to complement carotenoid biosynthesis. In other cases, the GGDP activities of these enzymes was demonstrated by *in vitro* assay after expression in *E. coli*, but the assays were performed with crude *E. coli* extracts without purification of the expressed proteins (Zhu *et al.*, 1997a,b; Okada *et al.*, 2000), creating background products that may have interfered with GFDP detection. In the present work, the IDS assay was performed using proteins with a GST tag expressed in *E. coli*, and purified from the crude extract using a glutathione sepharose column. The formation of GFDP by these *A. thaliana* IDSs was confirmed by several additional lines of evidence. First, use of either a His tag (Figure S6) or a GST tag (Figures 1 and 3) resulted in enzymes producing GFDP. Second, expression in *A. thaliana* also resulted in GFDP formation (Figure 4). Finally, we showed that extracts of wild-type roots have the ability to produce GFDP, and GFDP metabolite pools were detected in the roots themselves (Figure 7). Previous work had demonstrated that the genes encoding these GFDP synthases are predominantly expressed in roots, based on quantitative RT–PCR, microarray data and use of promoter–GUS fusion constructs (Beck *et al.*, 2013).

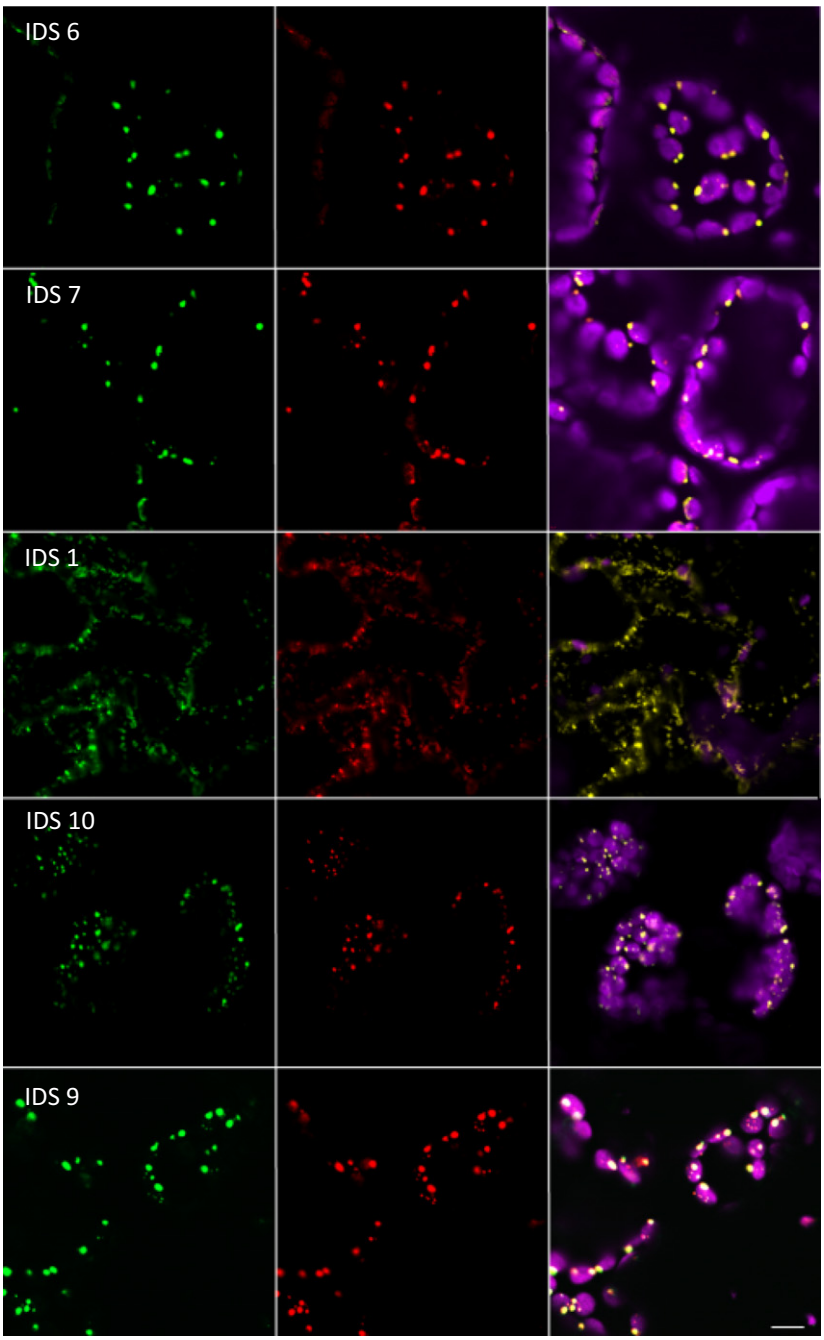

Figure 5. Subcellular localization of IDS–GFP fusion proteins.
Confocal microscopy of *N. benthamiana* leaves expressing IDS::eGFP with *At*PSY::mCherry (IDS 6, 7, 9, and 10) or with a mitochondrial mCherry marker (IDS1). The first column shows the eGFP signal, the second column shows the mCherry signal, and the third shows overlays of the eGFP and mCherry signals, with chlorophyll fluorescence in magenta. Scale bar = 10 μm.

For the previously described IDS from Archaea that produce GFDP, no kinetic measurements have been reported. However, when comparing the GFDP-producing *At*IDS9 with the characterized GGDP synthases from *Capsicum annum*, *Sinapsis alba* and *Saccharomyces cerevisiae*, similar kinetic parameters were observed for DMADP (Dogbo and Camara, 1987; Laferrière and Beyer, 1991; Lo *et al.*, 2009). In the same way, the pattern of lower K_m values for longer diphosphate substrates was also reported for the GGDP synthases from *Nicotiana tabacum* and *Taxus canadensis* (Burke and Croteau, 2002; Orlova *et al.*, 2009).

The presence of smaller amino acid residues at positions near the first aspartate-rich motif promotes GFDP formation

Structure–activity studies of IDSs have centered on the first aspartate-rich motif (FARM), which is involved in substrate binding. For FARMs of the DDxxxxD type, as in *A. thaliana*, substitution at the 5th amino acid N–terminal to the FARM

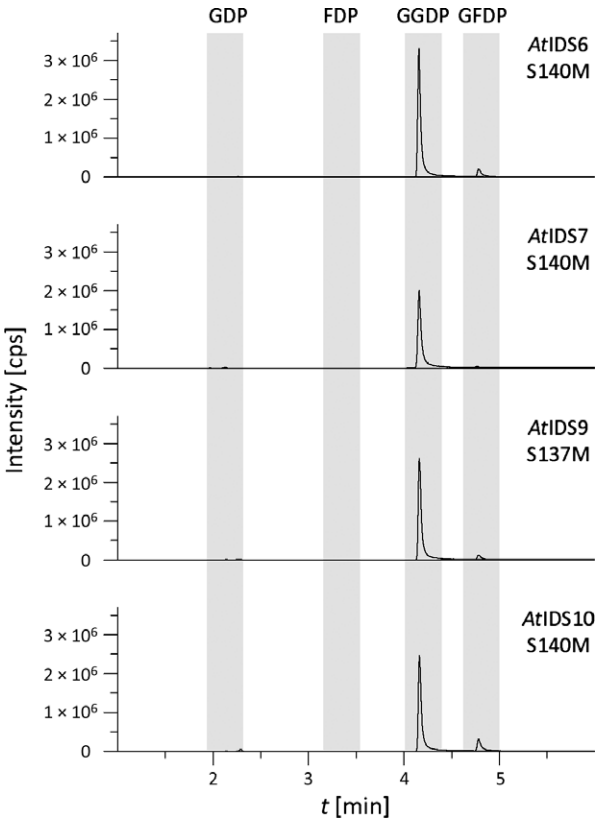

Figure 6. The 5th residue before the FARM motif is critical for GFDP activity.
A. thaliana IDS6, IDS7, IDS9 and IDS10 were mutated at the 5th residue before the first aspartate-rich motif (position 175, Figure 2) such that the Ser residue characteristic of these GFDP-forming IDS was altered to Met, which is characteristic of GGDP-forming IDS in *A. thaliana*. LC-MS/MS chromatograms are presented, showing the *in vitro* enzyme activities of mutated S175M *At*IDS6 (*At*3g14530), *At*IDS7 (*At*3g14550), *At*IDS9 (*At*3g29430) and *At*IDS10 (*At*3g32040) heterologously expressed in *E. coli* as GST fusion constructs and purified using glutathione sepharose columns. At least three replicate assays were performed for each construct with similar results.

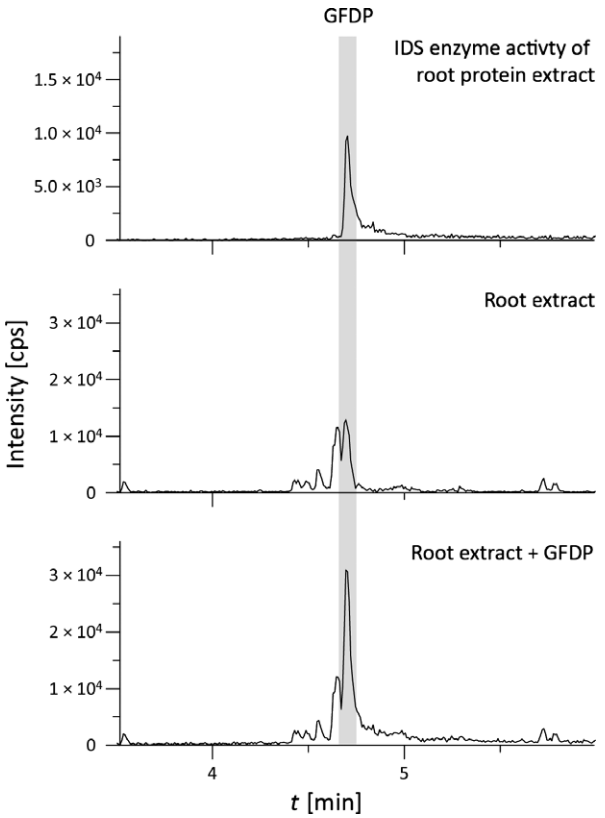

Figure 7. GFDP formation is detected in *A. thaliana* roots.
Top: total protein extracts of roots were assayed for synthesis of GFDP activity from IDP and DMADP. Middle and bottom: LC-MS/MS chromatograms of root extracts purified by solid-phase extraction were either untreated or spiked with authentic GFDP. Only the MRM trace for GFDP is shown.

influences product distribution, with larger residues limiting space for isoprenyl chain expansion and thus shortening the product (Wang and Ohnuma, 2000; Liang *et al.*, 2002). Consistent with this finding, we demonstrated here that the presence of the large amino acid residue Met resulted in a smaller product, GGDP (C_{20}), while the presence of the smaller amino acid residues Ala and Ser preferentially resulted in the larger product GFDP (C_{25}). Moreover, mutation of Ser to Met switched the product spectrum to the smaller compound (GGDP). Putative GFDP synthases still awaiting discovery in plants may also possess Ser, Ala or another small residue at this position, five amino acids N–terminal to the FARM. The results fit with previous work on a bacterial IDS from *Pantoea ananatis* with Ala at the 5th position, which produces mostly GGDP with some GDFP (Noike *et al.*, 2008). Mutation of this Ala to a larger residue, such as Phe, Leu or His, decreased the chain length of the product to GGDP or FDP. In another study, a bacterial IDS with Tyr at the 5th position that produced GGDP was converted to GFDP production by changing the Try to Ala, Gly, Cys or Ser (Ohnuma *et al.*, 1996). Among GFDP-forming IDSs from the Archaea, the FARM is of the DDxxD type, and the 8th position N–terminal to the FARM appears to be more important for product determination than the 5th residue. Mutational studies that converted the Met at this position into Ala resulted in a change in product from GFDP to GGDP (Ogawa *et al.*, 2011).

Multiple subcellular locations of GFDP synthases suggest multiple pools of GFPP

C–terminal GFP fusions show that *At*IDS1 is localized to the mitochondria and that *At*IDS 6, 7, 9 and 10 are localized to the plastids. This indicates that there are at least two distinct pools of GFDP in the cell. The existence of sesterterpenes in plants (see below) suggests that at least one of these pools is used for biosynthesis of these C_{25} terpenoids. Because, to the best of our knowledge, no plant

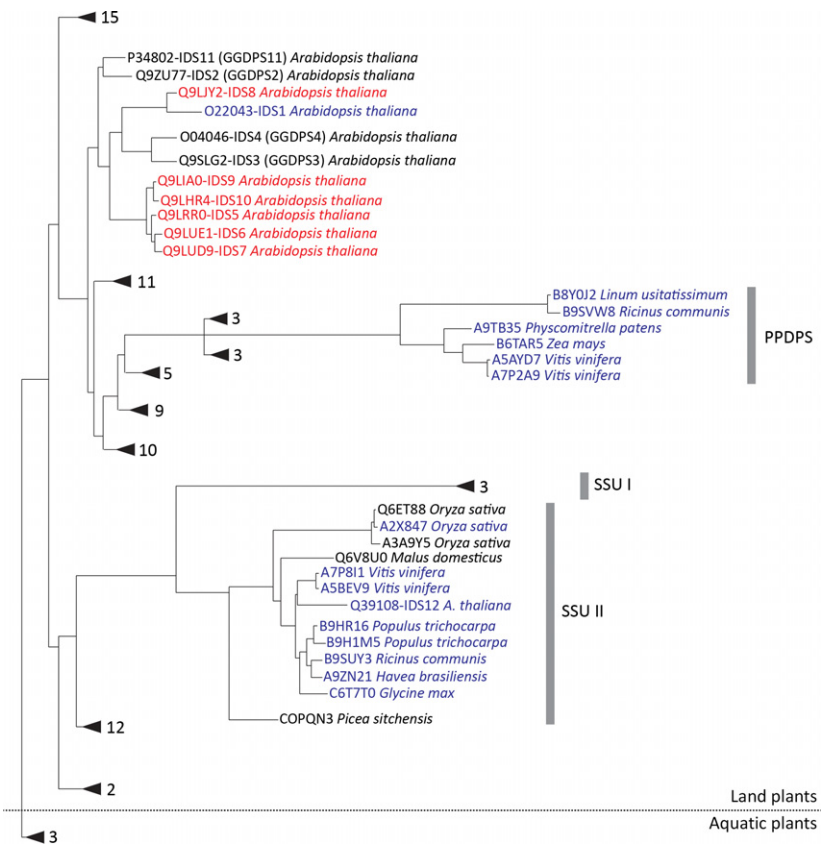

Figure 8. Phylogenetic tree of plant *trans*-IDS enzymes producing C20 or longer prenyl diphosphates, highlighting branches producing longer products.
As the presence of an Ala or Ser residue at the 5th residue before the FARM motif instead of the typical Met was shown to confer GFDP activity on enzymes of the GGDP group, only branches containing Ala or Ser are shown. Other branches are collapsed, and only the number of sequences for them are given. The phylogenetic tree was modified from that created by Coman *et al.* (2014). The Uniprot accession numbers of sequences with Ala at the 5th position N–terminal to the FARM are shown in blue, and those with Ser at the 5th position N–terminal to the FARM are shown in red. PPDPS, polyprenyl diphosphate synthase; SSU, small subunit.

terpene synthase has yet been found to be localized in the mitochondria of a native plant, it seems more likely that the plastidial pool acts in biosynthesis of sesterterpenes. There are a number of as yet uncharacterized Arabidopsis terpene synthases with predicted plastidic transit peptides, which represent potential candidates for the biosynthesis of sesterterpenes. The possible fate of GFDP in the mitochondria is unknown. One striking observation is the site of localization of *At*IDS 6, 7, 9 and 10 within the plastids and the co-occurrence of these enzymes with PSY. Whether these sites are indeed plastoglobules is still a matter of debate (Pasare *et al.*, 2013). Nonetheless, this sub-organellar distribution of GFDP synthases contrasts with that of *At*IDS11, the major GGDP synthase in Arabidopsis, which has a stromal localization (Beck *et al.*, 2013). Such spatial segregation of IDSs with distinct products may allow independent regulation of isoprenyl diphosphates for specific purposes. It should also be noted that plastoglobules are present in roots (Piller *et al.*, 2012), where *At*IDS6, 7, 9 and 10 are mostly expressed. Thus the localization in leaf plastoglobules may be relevant for roots, and suggests that the sub-organellar distribution of IDSs within plastids may direct fluxes of isoprenoid to distinct classes of isoprenoids. This direction of flux may explain the fact that over-expression of the GFDP synthase *At*IDS9 in leaves, which is targeted to plastids, gave rise to bleaching (Figure S3). Reduction in leaf pigments is probably a consequence of diversion of plastidial GGDP to GFDP instead of its use in the formation of carotenoids or the phytol side chain of chlorophyll. The root location of *At*IDS9 and other GFDP synthases (Beck *et al.*, 2013; Coman *et al.*, 2014) may avoid competition for GGDP with carotenoid and chlorophyll formation.

GFDP synthases are likely to be involved in sesterterpene formation

GFDP-forming IDSs may have diverse metabolic roles. In Archaea, these enzymes are thought to be involved in the biosynthesis of prenol lipids for membranes (Tachibana, 1994; Tachibana *et al.*, 2000; Ogawa *et al.*, 2010). In *A. thaliana* roots, they are probably involved in producing substrate for one of the uncharacterized root-localized terpene synthases (Chen *et al.*, 2003; Tholl and Lee, 2011) that produce a C_{25} sesterterpene product that accumulates or is further metabolized.

Sesterterpenes have been identified in nature largely in marine sponges, where they have anti-bacterial, anti-mollusk and fish-deterrent activities, and thus probably serve in defense against predators and pathogens (Ebada *et al.*, 2010). Their presence has also been shown in insects (Rios *et al.*, 1974; Veloz *et al.*, 1975; Kusumi *et al.*, 1979), fungi (Wang *et al.*, 1998, 2013; Cueto *et al.*, 2002; Nihashi *et al.*,

2002; Chiba *et al.*, 2013), bacteria (Sato *et al.*, 2013; Shinozaki *et al.*, 2013) and plants of the Solanaceae (Toyoda *et al.*, 1969; McDowell *et al.*, 2011) and Lamiaceae (Dal Piaz *et al.*, 2010; Luo *et al.*, 2010), as well as in *Gossypium hirsutum* (Malvaceae; Stipanovic *et al.*, 1977), *Croton hieronymi* (Euphorbiaceae; Catalan *et al.*, 2003) and *Aletris farinosa* (Liliaceae; Challinor *et al.*, 2013). When the roles of these sesterterpenes were investigated, they were also shown to function in protection against predators and pathogens. The broad distribution of sesterterpenes reported indicates a corresponding broad distribution of GFDP-forming IDSs, justifying increasing interest in these enzymes.

EXPERIMENTAL PROCEDURES

Plant material

Arabidopsis thaliana (Col–0) and IDS over-expressing lines were grown from seeds in a climate chamber (22°C, 55% relative humidity and 100 μmol m^{-2} sec^{-1} photosynthetically active radiation) under long-day conditions (16 h light/8 h dark) until flowers developed. For quantification of GFDP-producing activity and GFDP presence *in planta*, seedlings were grown in a mixture of sand and expanded clay aggregate.

Chemicals

Isopentenyl diphosphate, dimethylallyl diphosphate, geranyl diphosphate, farnesyl diphosphate, geranylgeranyl diphosphate, ammonium bicarbonate, methanol and acetonitrile (LC-MS grade) were purchased from Sigma-Aldrich (www.sigmaaldrich.com).

Syntheses

Geranylfarnesyl bromide. Tetrabromomethane (2.05 g, 6.19 mmol) and triphenylphosphine (1.62 g, 6.19 mmol) were added to a solution of geranylfarnesol (1.85 g, 5.16 mmol) in dichloromethane (25 ml) at 0°C. After 1 h stirring, *n*–hexane (200 ml) was added. The precipitate was filtered off, and the filtrate was concentrated under reduced pressure. Purification of the residue was performed by flash chromatography on silica (*n*–hexane/methyl *tert*-butyl ether, 20:1), yielding geranylfarnesyl bromide (1.99 g, 4.72 mmol, 91%) as a colorless oil: ^{1}H NMR (400 MHz, $CDCl_3$): δ = 5.53 (t, *J* = 8.4 Hz, 1H), 5.16 – 5.04 (m, 4H), 4.02 (d, *J* = 8.4 Hz, 2H), 2.16 – 1.94 (m, 16H), 1.73 (s, 3H), 1.68 (s, 3H), 1.60 ppm (s, 12H); ^{13}C NMR (101 MHz, $CDCl_3$): δ = 143.57, 135.63, 134.96, 134.88, 131.21, 124.39, 124.22, 124.17, 123.36, 120.53, 39.71, 39.70, 39.67, 39.52, 29.63, 26.76, 26.65, 26.61, 26.09, 25.68, 17.67, 16.05, 16.01, 16.00, 15.96 ppm.

Geranylfarnesyl diphosphate (GFDP). *N*,*N*–di-isopropylethylamine (2.40 ml, 14.09 mmol) and a mixture of acetone (1.10 ml, 14.95 mmol) and water (154 μl, 8.54 mmol) were added to tetrakis (trimethylsilyl) diphosphate (9.96 g, 21.35 mmol) at 0°C (Wessjohann and Dessoy, 2004, 2014). After 10 min stirring, geranylfarnesyl bromide (1.80 g, 4.27 mmol) was added, and the reaction mixture was left for additional 24 h at room temperature without stirring. Subsequently, the liquid phase was separated from the crystals formed, and added to a stirred ammonium hydroxide solution (6 M, 20 ml) at 0°C. The resulting solution was washed three times with 20 ml diethyl ether for 1 min at room temperature. Then ethanol (200 ml) was added under vigorous stirring. The precipitate formed was filtered off, and the filtrate was concentrated to less than 5 ml. Ammonium hydroxide solution (6 M, 5 ml) and acetonitrile (200 ml) were then added to the stirred solution. The precipitate was filtered off and dissolved in ammonium hydroxide solution (10 ml). The resulting solution was lyophilized, yielding geranylfarnesyl diphosphate as the corresponding trisammonium salt (379 mg, 665 μmol, 16%) as a white solid: ^{1}H NMR (400 MHz, D_2O + CD_3OD + ND_4OD): δ = 5.43 (m, 1H), 5.19 – 5.00 (m, 4H), 4.46 (m, 2H), 2.22 – 1.81 (m, 16H), 1.71 (s, 3H), 1.63 (s, 3H), 1.59 (s, 3H), 1.57 (s, 3H), 1.56 ppm (s, 6H); ^{13}C NMR (101 MHz, D_2O + CD_3OD + ND_4OD): δ = 144.05, 137.85, 137.24, 137.07, 133.20, 127.28, 127.15, 127.12, 126.80, 123.13 (m), 65.23 (d, *J* = 5.3 Hz), 42.70, 42.60, 42.54, 42.49, 29.78, 29.58, 29.56, 29.49, 28.22, 20.15, 18.81, 18.57, 18.54, 18.48 ppm; ^{31}P NMR (162 MHz, D_2O + CD_3OD + ND_4OD): −6.79 (br), −10.10 ppm (br); MS/ESI: *m/z* = 517.6 ([M-$2NH_3$-NH_4]$^-$, 100%), 1035.0 ([2M-$5NH_3$-NH_4]$^-$, 21%); HRMS/ESI: calculated for $C_{25}H_{43}O_7P_2$: 517.2489 [M-$2NH_3$-NH_4]$^-$, found: 517.2481.

Heterologous expression of IDS in E. coli

Cloning, transformation and expression. The truncated GST–IDS fusion constructs as described by Beck *et al.* (2013) were used. Additionally *At*IDS7 and the *At*IDS small subunit were cloned from cDNA into the C–terminal His tag-containing pET–101 vector (Life Technologies, www.lifetechnologies.com) according to the manufacturer's instructions. Primers are shown in Table S2. For expression, all vectors were transformed into *E. coli* BL21 (DE3) pLysS (Life Technologies). Cultures were grown in 100 ml of liquid LB medium at 18°C and 200 rpm. Expression was induced using the Overnight Express AutoInduction System 1 (Merck Millipore, www.emdmillipore.com). Bacterial pellets were resuspended in 3 ml 25 mM 3–(*N*-morpholino)-2–hydroxypropanesulfonic acid (MOPSO), pH 7.2, 10 mM $MgCl_2$, 10% v/v glycerol, and purified using 0.2 ml glutathione spin columns (Thermo Fisher Scientific, www.piercenet.com) for GST-tagged proteins, or Ni–NTA spin columns (Qiagen, www.qiagen.com) for His-tagged proteins, according to the manufacturer's instructions.

Assay and product analysis. Enzyme assays were performed using 1 μg of purified heterologously expressed protein (or 10 μg of total protein for *A. thaliana* extractions) in 200 μl of 25 mM MOPSO buffer at pH 7.2 with 10% v/v glycerol and 10 mM $MgCl_2$, and 50 μM IDP and 50 μM DMADP (both Sigma-Aldrich) as substrates. After incubation for 1 h at 30°C, identification and quantification were performed as described by Nagel *et al.* (2014) with the addition of multiple reaction monitoring (MRM) of *m/z* 517 to 79 for GFDP. Quantification of the product ratios was performed using external calibration curves. Data analysis was performed using Analyst Software 1.6, build 3773 (AB Sciex, www.sciex.com).

Heterologous expression in N. benthamiana

Cloning. For cytosolic expression of *At*IDS9 in *N. benthamiana*, the predicted transit peptide (first 81 bp according to http://www.cbs.dtu.dk/services/TargetP/) was removed. The sequences were amplified from *A. thaliana* (Col–0) root cDNA, and *Bsa*I and *Bpi*I restriction sites were removed from the IDS9 sequence by dividing the gene sequence into sub-fragments. Oligonucleotide sequences are listed in Table S2. Fragments were cloned into the pAGM1311 vector (Engler *et al.*, 2014), and sequenced before cloning the truncated sequence of *At*IDS9 into the pAGM1287 vector (Engler *et al.*, 2014). In the final cloning step, the IDS9 sequence was further fused to an N–terminal 6xHis tag in a tobacco mosaic virus-based vector containing a RdRp gene with 16 introns (vector pICH18722, as described by Marillonnet *et al.*,

2005) to allow for RNA amplification and increased gene expression. The viral vector is under the control of the *A. thaliana Act2* promoter, and was cloned into the T–DNA vector pICH75044 (Engler *et al.*, 2014).

Transformation, expression and purification. *Agrobacterium tumefaciens* strain GV3101 (pMP90) was transformed with IDS9 recombinant plasmids, with cultivation of agrobacteria and infiltration of *N. benthamiana* leaves being performed as described previously (Brückner *et al.*, 2014). After transformation, the plants were returned for 6 days to the growth chamber before leaf material was harvested and frozen in liquid nitrogen, and 300 mg was ground with mortar and pestle to a fine powder. Purification of the His_6-tagged *At*IDS9 protein was performed using Ni–NTA magnetic agarose beads (Qiagen), according to the manufacturer's instructions. After purification, size exclusion filters (Amicon Ultra–4, 10 K, www.merckmillipore.com) were used to enrich the protein concentration while exchanging the imidazole-rich buffer from the purification step with the enzyme assay buffer (25 mM MOPSO, pH 7.2, 10 mM $MgCl_2$ and 10% v/v glycerol).

Kinetic assays and product analysis. For determination of apparent kinetic constants, eight concentrations each of the substrates DMADP (0–100 μM), GDP (0–50 μM), FDP (0–50 μM) or GGDP (0–50 μM) were used in the presence of a fixed IDP concentration (100 μM). The assay mixtures contained 25 mM MOPSO (pH 7.2), 10 mM $MgCl_2$ and 10% v/v glycerol, plus IDP and DMADP, GDP, FDP or GGDP and 1 μg purified *At*IDS9 per assay in a 200 μl volume. The reaction mixture was incubated in glass vials at 20°C for times ranging from 0–2 min in 10 sec intervals with shaking using an Eppendorf Thermomixer® Comfort (www.eppendorf.com), and the reaction was stopped by immediately freezing the sample in liquid nitrogen. To determine the GFDP concentration, samples were analyzed via UPLC/MS using a calibration curve. All MS analyses were performed on an AB Sciex Q–Trap 6500 mass spectrometer connected to a Waters Aquity UPLC (www.waters.com), and data were collected and analyzed using Analyst 1.6.2 software (Sciex, www.sciex.com). Separation was accomplished using a Macherey–Nagel Nucleoshell Hilic 2.7 μm UPLC column (150 mm × 2 mm). The injection volume was 5 μl. A solvent system was used containing solution A (20 mM ammonium formate in water, pH 2.5) and solution B (20 mM ammonium formate in 95:5 acetonitrile/water, pH 4) with the following gradient: 0–1.5 min isocratic with 100% B, 1.5–9 min linear from 100% to 30% B, 9–11 min isocratic with 30% B, 11–12 min linear from 30% to 100% B, and 12–14 min isocratic with 100% B. The flow rate was 400 μl min^{-1} and the column temperature was 40°C. After each injection, the injection needle was washed with 1.5 ml 10 mM ammonium formate in 80:20 methanol/water, pH 4, and 600 μl acetonitrile. Mass spectrometric data were recorded in MRM mode (Table S3) with negative ionization. Peak area integration was performed using the AB Sciex program Multiquant version 3.0.5373.0.

Subcellular localization. For cloning of C–terminal eGFP (IDS 1, 6, 8, 9 and 10) and mCherry fusions (Arabidopsis phytoene synthase, At5g17230), the Golden Gate cloning method (Engler *et al.*, 2008) was use. Oligonucleotide sequences are provided in Table S2. The predicted transit peptide according to ChloroP (http://www.cbs.dtu.dk/services/ChloroP/) was amplified from cDNA from *A. thaliana* Col–0 roots, and the rest of the coding sequence was amplified from expression vectors that contain the truncated IDS sequence (see above). Prior to cloning, removal of any *Bpi*I and *Bsa*I restriction sites that were present within the IDS gene sequences was performed as described by Engler *et al.* (2008). IDS fragments were cloned into the pAGM1311 vector (Engler *et al.*, 2014), and gene sequences for the *At*IDS9 transit peptide deletion study were cloned into the pUC18 vector (Thermo, www.thermofisher.com) by a single restriction/ligation reaction using *Bsa*I and T4 ligase and sequenced. The full-length coding sequences of the *AtIDS1*, *6*, *9* and *10* genes were then cloned into the pAGM1287 vector (Engler *et al.*, 2014). In the last cloning step, the IDS coding sequences and the gene sequences for the IDS9 transit peptide deletion study were fused to a C–terminal eGFP tag under the control of the CaMV 35S promoter and with the Ocs terminator, and cloned into T–DNA vector pICH75044 (Engler *et al.*, 2014). *A. tumefaciens* strain GV3101 was transformed with *IDS::eGFP*- or *PSY::mCherry*-containing recombinant plasmids as described previously (Brückner *et al.*, 2014). The mitochondrial marker (mCherry fusion protein) has been described previously (Nelson *et al.*, 2007).

Over-expression in A. thaliana

Coding sequences of the *A. thaliana* genes *At*IDS9 (S175) and *At*IDS11 (M175) were amplified from total Arabidopsis cDNA using the oligonucleotide sequences given in Table S2, and cloned into the Gateway-compatible pENTR/D–TOPO entry vector (Invitrogen, http://www.invitrogen.com), resulting in the pENTR/D–TOPO-IDS9 and pENTR/D–TOPO-IDS112 vectors. Constructs were checked by DNA sequencing. LR reactions were then performed to clone these cDNAs into the binary pK7WG2.0 vector (http://gateway.psb.ugent.be; Karimi *et al.*, 2005). The resulting constructs (pIDS9 and pIDS11) consisted of the IDS genes under the control of the CaMV 35S promoter. Constructs were introduced into *A. tumefaciens* strain C58C1 (pMP90) (Koncz and Shell, 1986), and then into wild-type Arabidopsis plants via the floral-dip method (Clough and Bent, 1998). Primary transformants were selected on MS medium supplemented with kanamycin (50 μg ml^{-1}).

Complementation of the AtIDS11 loss-of-function mutant by AtIDPS isoforms

The heterozygous *At*IDPS11 loss-of-function embryo-lethal *A. thaliana* mutant (*ggpps11–4*, SAIL_712_D06; Ruiz-Sola *et al.*, 2015) was transformed using *A. thaliana* genes *At*IDS1 (*At*1g49530), AtIDS2 (*At*2g18620), *At*IDS6 (*At*3g14530), *At*IDS7 (*At*3g14550), *At*IDS9 (*At*3g29430), *At*IDS10 (*At*3g32040) and *At*IDS11 (*At*4g36810) under the control of the native *At*IDS11 promoter. The individual *At*IDS genes were cloned into the binary pK7WG2.0 vector by Gateway technology in similar way to that described above, e.g. via pENTR/D-TOPO cloning and LR reaction. GGDPS-/comp primers were used to amplify GGDPS (Table S2). Then the original CaMV 35S promoter was cut out by digestion with *Spe*I/*Sal*I and replaced by an *Spe*I/*Xho*I restriction fragment of the *At*IDS11 promoter. The sequences of primers used for cloning are listed in Table S2. Primary transgenic plants (T_1) were selected on MS medium supplemented with 1% w/v sucrose, phosphinotricin (40 μg ml^{-1}) and kanamycin (50 μg ml^{-1}).

Site-directed mutagenesis

Specific nucleotides of IDS–GST fusion constructs were mutated using a Q5 site-directed mutagenesis kit (New England Biolabs, www.neb-online.de) according to the manufacturer's instructions. Primers are listed in Table S2. The resulting vector constructs

were checked for successful mutation by sequencing. Expression was performed in *E. coli* as described above.

Preparation of protein extracts from A. thaliana

Protein extraction was performed as described by Nagel *et al.* (2012). Plant tissue was ground with a mortar and pestle under liquid nitrogen by hand to a fine powder. Cooled extraction buffer was added to frozen tissue at a ratio of 5:1 buffer:tissue (ml g^{-1}). The extraction buffer contained 250 mM MOPSO (pH 6.8), 5 mM ascorbic acid, 5 mM sodium bisulfite, 5 mM dithiothreitol, 10 mM $MgCl_2$, 1 mM EDTA, 10% v/v glycerol, 1% w/v polyvinylpyrrolidone (M_r = 10 000), 4% w/v polyvinylpolypyrrolidone, 4% w/v Amberlite XAD–4 (Sigma-Aldrich) and 0.1% v/v Tween–20. Extraction was performed in Eppendorf Protein LoBind tubes with an Eppendorf Thermomixer at 4°C and 1400 rpm for 30 min. After centrifugation for 20 min at 4°C and 20 000 *g*, the supernatant was passed through a 2 ml Zeba Spin desalting column with a 7 kDa molecular weight cut-off (Thermo Scientific) to exchange the buffer with 25 mM MOPSO (pH 7.2), 10 mM $MgCl_2$, 10% (v/v) glycerol, according to the manufacturer's instructions. The protein concentration was determined using the Protein Assay Dye Reagent Concentrate (Bio–Rad, www.bio-rad.com) with BSA (Bio–Rad) as standard. Assays and product quantification were performed as described in Nagel et al. (2014) with an injection volume of 1 μl and without MRMs for the internal standards GSDP and FSDP.

Extraction of prenyl diphosphates from A. thaliana

A 0.5 g portion of ground root tissue was extracted and quantified as described by Nagel *et al.* (2014), except that the eluent from the solid-phase-extraction column was dissolved in 300 μl water/methanol (1:1) after evaporation.

ACKNOWLEDGMENTS

We thank Marion Stäger, Anne Brückner and Mareike Bock for help with protein expression and GST purification, Diana Kopcsayová (Institute of Biology and Ecology, Pavol Jozef Safarik University Kosice, Slovakia) for help with the complementation studies, and the Max Planck Society, the Zwillenberg–Tietz Foundation, and grant 1/0417/13 from the Scientific grant agency of the Slovak Ministry of Education, Science, Research and Sport and of the Slovak Academy of Sciences for support (for Eva Vranova).

SUPPORTING INFORMATION

Additional Supporting Information may be found in the online version of this article.

Figure S1. *A. thaliana* IDS2 and IDS11 have GGDP synthase activity.

Figure S2. Lineweaver–Burk plots for calculation of apparent *in vitro* K_m values for *At*IDS9 with various substrates.

Figure S3. Morphology of *A. thaliana* Col–0 wild type and lines over-expressing *At*IDS9 or *At*IDS11.

Figure S4. Complementation of the *A. thaliana At*IDS11 mutant *ggpps11–4* with various *AtIDS* genes driven by the *AtIDS11* promoter.

Figure S5. Subcellular localization of truncated *At*IDS9–GFP fusion proteins.

Figure S6. *A. thaliana* IDS7 GFDP activity is not affected by the presence of *A. thaliana* IDS small subunit protein.

Figure S7. Prenyl diphosphate formation in *A. thaliana* roots.

Table S1. Product distribution of *At*IDS1, 6, 7, 9 and 10.

Table S2. List of primers used.

Table S3. MRM transitions used in LC-MS quantification.

REFERENCES

Aaron, J.A. and Christianson, D.W. (2010) Trinuclear metal clusters in catalysis by terpenoid synthases. *Pure Appl. Chem.*, **82**, 1585–1597.

Akhtar, T.A., Matsuba, Y., Schauvinhold, I., Yu, G., Lees, H.A., Klein, S.E. and Pichersky, E. (2013) The tomato *cis*–prenyltransferase gene family. *Plant J.*, **73**, 640–652.

Arigoni, D., Sagner, S., Latzel, C., Eisenreich, W., Bacher, A. and Zenk, M.H. (1997) Terpenoid biosynthesis from 1–deoxy-D–xylulose in higher plants by intramolecular skeletal rearrangement. *Proc. Natl Acad. Sci. USA*, **94**, 10600–10605.

Beck, G., Coman, D., Herren, E., Ruiz-Sola, M., Rodriguez-Concepcion, M., Gruissem, W. and Vranova, E. (2013) Characterization of the GGPP synthase gene family in *Arabidopsis thaliana*. *Plant Mol. Biol.*, **82**, 393–416.

Bouvier, F., Suire, C., d'Harlingue, A., Backhaus, R.A. and Camara, B. (2000) Molecular cloning of geranyl diphosphate synthase and compartmentation of monoterpene synthesis in plant cells. *Plant J.* **24**, 241–252.

Brückner, K., Bozic, D., Manzano, D., Papaefthimiou, D., Pateraki, I., Scheler, U., Ferrer, A., de Vos, R.C.H., Kanellis, A.K. and Tissier, A. (2014) Characterization of two genes for the biosynthesis of abietane-type diterpenes in rosemary (*Rosmarinus officinalis*) glandular trichomes. *Phytochemistry*, **101**, 52–64.

Burke, C. and Croteau, R. (2002) Interaction with the small subunit of geranyl diphosphate synthase modifies the chain length specificity of geranylgeranyl diphosphate synthase to produce geranyl diphosphate. *J. Biol. Chem.*, **277**, 3141–3149.

Burke, C., Klettke, K. and Croteau, R. (2004) Heteromeric geranyl diphosphate synthase from mint: construction of a functional fusion protein and inhibition by bisphosphonate substrate analogs. *Arch. Biochem. Biophys.*, **422**, 52–60.

Catalan, C.A.N., de Heluani, C.S., Kotowicz, C., Gedris, T.E. and Herz, W. (2003) A linear sesterterpene, two squalene derivatives and two peptide derivatives from *Croton hieronymi*. *Phytochemistry*, **64**, 625–629.

Challinor, V.L., Chap, S., Lehmann, R.P., Bernhardt, P.V. and De Voss, J.J. (2013) Structure and absolute configuration of methyl-(3R)-malonyl-(13S)-hydroxycheilanth-17–en-19–oate, a sesterterpene derivative from the roots of *Aletris farinosa*. *J. Nat. Prod.*, **76**, 485–488.

Chang, T.H., Hsieh, F.L., Ko, T.P., Teng, K.H., Liang, P.H. and Wang, A.H.J. (2010) Structure of a heterotetrameric geranyl pyrophosphate synthase from mint (*Mentha piperita*) reveals intersubunit regulation. *Plant Cell*, **22**, 454–467.

Chen, F., Tholl, D., D'Auria, J.C., Farooq, A., Pichersky, E. and Gershenzon, J. (2003) Biosynthesis and emission of terpenoid volatiles from Arabidopsis flowers. *Plant Cell*, **15**, 481–494.

Chiba, R., Minami, A., Gomi, K. and Oikawa, H. (2013) Identification of Ophiobolin F synthase by a genome mining approach: a sesterterpene synthase from *Aspergillus clavatus*. *Org. Lett.*, **15**, 594–597.

Closa, M., Vranová, E., Bortolotti, C., Bigler, L., Arró, M., Ferrer, A. and Gruissem, W. (2010) The *Arabidopsis thaliana* FPP synthase isozymes have overlapping and specific functions in isoprenoid biosynthesis and complete loss of FPP synthase activity causes early developmental arrest. *Plant J.*, **63**, 512–525.

Clough, S.J. and Bent, A.F. (1998) Floral dip: a simplified method for *Agrobacterium*-mediated transformation of *Arabidopsis thaliana*. *Plant J.*, **16**, 735–743.

Coman, D., Altenhoff, A., Zoller, S., Gruissem, W. and Vranova, E. (2014) Distinct evolutionary strategies in the GGPPS family from plants. *Front. Plant Sci.*, **5**, 230.

Cueto, M., Jensen, P.R. and Fenical, W. (2002) Aspergilloxide, a novel sesterterpene epoxide from a marine-derived fungus of the genus *Aspergillus*. *Org. Lett.*, **4**, 1583–1585.

Dal Piaz, F., Imparato, S., Lepore, L., Bader, A. and De Tommasi, N. (2010) A fast and efficient LC-MS/MS method for detection, identification and quantitative analysis of bioactive sesterterpenes in *Salvia dominica* crude extracts. *J. Pharm. Biomed. Anal.*, **51**, 70–77.

Degenhardt, J., Köllner, T.G. and Gershenzon, J. (2009) Monoterpene and sesquiterpene synthases and the origin of terpene skeletal diversity in plants. *Phytochemistry*, **70**, 1621–1637.

Dogbo, O. and Camara, B. (1987) Purification of isopentenyl pyrophosphate isomerase and geranylgeranyl pyrophosphate synthase from *Capsicum*

chromoplasts by affinity chromatography. *Biochim. Biophys. Acta*, **920**, 140–148.

Ebada, S.S., Lin, W.H. and Proksch, P. (2010) Bioactive sesterterpenes and triterpenes from marine sponges: occurrence and pharmacological significance. *Mar. Drugs*, **8**, 313–346.

Engler, C., Kandzia, R. and Marillonnet, S. (2008) A one pot, one step, precision cloning method with high throughput capability. *PLoS One*, **3**, e3647.

Engler, C., Youles, M., Gruetzner, R., Ehnert, T.M., Werner, S., Jones, J.D., Patron, N.J. and Marillonnet, S. (2014) A Golden Gate modular cloning toolbox for plants. *ACS Synth. Biol.*, **3**, 839–843.

Hsieh, F.L., Chang, T.H., Ko, T.P. and Wang, A.H.J. (2011) Structure and mechanism of an Arabidopsis medium/long-chain-length prenyl pyrophosphate synthase. *Plant Physiol.*, **155**, 1079–1090.

Karimi, M., De Meyer, B. and Hilson, P. (2005) Modular cloning in plant cells. *Trends Plant Sci.*, **10**, 103–105.

Koksal, M., Hu, H.Y., Coates, R.M., Peters, R.J. and Christianson, D.W. (2011) Structure and mechanism of the diterpene cyclase *ent*-copalyl diphosphate synthase. *Nat. Chem. Biol.*, **7**, 431–433.

Koncz, C. and Shell, C. (1986) The promoter of T1-DNA gene 5 controls the tissue-specific expression of chimaeric genes carried by novel type of *Agrobacterium* binary vector. *Mol. Gen. Genet.*, **204**, 383–396.

Kusumi, T., Kinoshita, T., Fujita, K. and Kakisawa, H. (1979) A new macrocyclic sesterterpene acid from *Ceroplastes ceriferus*. *Chem. Lett.*, **9**, 1129–1132.

Laferrière, A. and Beyer, P. (1991) Purification of geranylgeranyl diphosphate synthase from *Sinapis alba* etioplasts. *Biochim. Biophys. Acta*, **1077**, 167–172.

Liang, P.-H., Ko, T.-P. and Wang, A.H.-J. (2002) Structure, mechanism and function of prenyltransferases. *Eur. J. Biochem.*, **269**, 3339–3354.

Lo, C.H., Chang, Y.H., Wright, J.D., Chen, S.H., Kan, D., Lim, C. and Liang, P.H. (2009) Combined experimental and theoretical study of long-range interactions modulating dimerization and activity of yeast geranylgeranyl diphosphate synthase. *J. Am. Chem. Soc.*, **131**, 4051–4062.

Luo, S.H., Luo, Q.A., Niu, X.M., Xie, M.J., Zhao, X., Schneider, B., Gershenzon, J. and Li, S.H. (2010) Glandular trichomes of *Leucosceptrum canum* harbor defensive sesterterpenoids. *Angew. Chem. Int. Ed.*, **49**, 4471–4475.

Marillonnet, S., Thoeringer, C., Kandzia, R., Klimyuk, V. and Gleba, Y. (2005) Systemic *Agrobacterium tumefaciens*-mediated transfection of viral replicons for efficient transient expression in plants. *Nat. Biotechnol.*, **23**, 718–723.

McDowell, E.T., Kapteyn, J., Schmidt, A. *et al.* (2011) Comparative functional genomic analysis of *Solanum* glandular trichome types. *Plant Physiol.*, **155**, 524–539.

Nagel, R., Gershenzon, J. and Schmidt, A. (2012) Nonradioactive assay for detecting isoprenyl diphosphate synthase activity in crude plant extracts using liquid chromatography coupled with tandem mass spectrometry. *Anal. Biochem.*, **422**, 33–38.

Nagel, R., Berasategui, A., Paetz, C., Gershenzon, J. and Schmidt, A. (2014) Overexpression of an isoprenyl diphosphate synthase in spruce leads to unexpected terpene diversion products that function in plant defense. *Plant Physiol.*, **164**, 555–569.

Nelson, B.K., Cai, X. and Nebenführ, A. (2007) A multi-color set of *in vivo* organelle markers for colocalization studies in Arabidopsis and other plants. *Plant J.*, **51**, 1126–1136.

Nihashi, Y., Lim, C.H., Tanaka, C., Miyagawa, H. and Ueno, T. (2002) Phytotoxic sesterterpene, 11–epiterpestacin, from *Bipolaris sorokiniana* NSDR-011. *Biosci. Biotechnol. Biochem.*, **66**, 685–688.

Noike, M., Katagiri, T., Nakayama, T., Koyama, T., Nishino, T. and Hemmi, H. (2008) The product chain length determination mechanism of type II geranylgeranyl diphosphate synthase requires subunit interaction. *FEBS J.*, **275**, 3921–3933.

Ogawa, T., Yoshimura, T. and Hemmi, H. (2010) Geranylfarnesyl diphosphate synthase from *Methanosarcina mazei*: different role, different evolution. *Biochem. Biophys. Res. Commun.*, **393**, 16–20.

Ogawa, T., Yoshimura, T. and Hemmi, H. (2011) Connected cavity structure enables prenyl elongation across the dimer interface in mutated geranylfarnesyl diphosphate synthase from *Methanosarcina mazei*. *Biochem. Biophys. Res. Commun.*, **409**, 333–337.

Ohnuma, S., Hirooka, K., Hemmi, H., Ishida, C., Ohto, C. and Nishino, T. (1996) Conversion of product specificity of archaebacterial geranylgeranyl-diphosphate synthase – identification of essential amino acid residues for chain length determination of prenyltransferase reaction. *J. Biol. Chem.*, **271**, 18831–18837.

Okada, K., Saito, T., Nakagawa, T., Kawamukai, M. and Kamiya, Y. (2000) Five geranylgeranyl diphosphate synthases expressed in different organs are localized into three subcellular compartments in Arabidopsis. *Plant Physiol.*, **122**, 1045–1056.

Orlova, I., Nagegowda, D.A., Kish, C.M. *et al.* (2009) The small subunit of snapdragon geranyl diphosphate synthase modifies the chain length specificity of tobacco geranylgeranyl diphosphate synthase *in planta*. *Plant Cell*, **21**, 4002–4017.

Pasare, S., Wright, K., Campbell, R., Morris, W., Ducreux, L., Chapman, S., Bramley, P., Fraser, P., Roberts, A. and Taylor, M. (2013) The sub-cellular localisation of the potato (*Solanum tuberosum* L.) carotenoid biosynthetic enzymes, CrtRb2 and PSY2. *Protoplasma*, **250**, 1381–1392.

Piller, L.E., Abraham, M., Dörmann, P., Kessler, F. and Besagni, C. (2012) Plastid lipid droplets at the crossroads of prenylquinone metabolism. *J. Exp. Bot.*, **63**, 1609–1618.

Rios, T., Quijano, L. and Calderon, J. (1974) Albolineol, a sesterterpene with a novel bicyclic skeleton. *J. Chem. Soc., Chem. Commun.*, **18**, 728–729.

Rodríguez-Concepción, M. (2006) Early steps in isoprenoid biosynthesis: multilevel regulation of the supply of common precursors in plant cells. *Phytochem. Rev.*, **5**, 1–15.

Ruiz-Sola, M.A., Coman, D., Beck, G. *et al.* (2015) *Arabidopsis* geranylgeranyl diphosphate synthase 11 is a hub isozyme required for the production of most photosynthesis-related isoprenoids. *New Phytol.* doi:10.1111/nph.13580. [Epub ahead of print].

Sallaud, C., Rontein, D., Onillon, S. *et al.* (2009) A novel pathway for sesquiterpene biosynthesis from *Z*, *Z*-farnesyl pyrophosphate in the wild tomato Solanum habrochaites. *Plant Cell*, **21**, 301–317.

Sato, T., Yamaga, H., Kashima, S., Murata, Y., Shinada, T., Nakano, C. and Hoshino, T. (2013) Identification of novel sesterterpene/triterpene synthase from *Bacillus clausii*. *ChemBioChem*, **14**, 822–825.

Schilmiller, A.L., Schauvinhold, I., Larson, M., Xu, R., Charbonneau, A.L., Schmidt, A., Wilkerson, C., Last, R.L. and Pichersky, E. (2009) Monoterpenes in the glandular trichomes of tomato are synthesized from a neryl diphosphate precursor rather than geranyl diphosphate. *Proc. Natl Acad. Sci. USA*, **106**, 10865–10870.

Schmidt, A., Wächtler, B., Temp, U., Krekling, T., Seguin, A. and Gershenzon, J. (2010) A bifunctional geranyl and geranylgeranyl diphosphate synthase is involved in terpene oleoresin formation in *Picea abies*. *Plant Physiol.*, **152**, 639–655.

Shinozaki, J., Shibuya, M., Ebizuka, Y. and Masuda, K. (2013) Cyclization of all-*E*- and 2*Z*-geranylfarnesols by a bacterial triterpene synthase: insight into sesterterpene biosynthesis in *Aleuritopteris* ferns. *Biosci. Biotechnol. Biochem.*, **77**, 2278–2282.

Shumskaya, M., Bradbury, L.M., Monaco, R.R. and Wurtzel, E.T. (2012) Plastid localization of the key carotenoid enzyme phytoene synthase is altered by isozyme, allelic variation, and activity. *Plant Cell*, **24**, 3725–3741.

Stipanovic, R.D., Bell, A.A., Obrien, D.H. and Lukefahr, M.J. (1977) Heliocide H–2 insecticidal sesterterpenoid from cotton (*Gossypium*). *Tetrahedron Lett.*, **6**, 567–570.

Tachibana, A. (1994) A novel prenyltransferase, farnesylgeranyl diphosphate synthase, from the haloalkaliphilic archaeon, *Aatronobacterium pharaonis*. *FEBS Lett.*, **341**, 291–294.

Tachibana, A., Yano, Y., Otani, S., Nomura, N., Sako, Y. and Taniguchi, M. (2000) Novel prenyltransferase gene encoding farnesylgeranyl diphosphate synthase from a hyperthermophilic archaeon, *Aeropyrum pernix* – molecular evolution with alteration in product specificity. *Eur. J. Biochem.*, **267**, 321–328.

Tholl, D. (2006) Terpene synthases and the regulation, diversity and biological roles of terpene metabolism. *Curr. Opin. Plant Biol.*, **9**, 297–304.

Tholl, D. and Lee, S. (2011) Terpene specialized metabolism in *Arabidopsis thaliana*. *Arabidopsis Book*, **9**, e0143.

Tholl, D., Kish, C.M., Orlova, I., Sherman, D., Gershenzon, J., Pichersky, E. and Dudareva, N. (2004) Formation of monoterpenes in *Antirrhinum majus* and *Clarkia breweri* flowers involves heterodimeric geranyl diphosphate synthases. *Plant Cell*, **16**, 977–992.

Toyoda, M., Asahina, M., Fukawa, H. and Shimizu, T. (1969) Isolation of new acyclic C25-isoprenyl alcohol from potato leaves. *Tetrahedron Lett.*, **55**, 4879–4882.

Veloz, R., Quijano, L., Calderon, J.S. and Rios, T. (1975) Albocerol, a new macrocyclic sesterterpene. *J. Chem. Soc., Chem. Commun.*, **6**, 191–192.

Vranová, E., Coman, D. and Gruissem, W. (2013) Network analysis of the MVA and MEP pathways for isoprenoid synthesis. *Annu. Rev. Plant Biol.*, **64**, 665–700.

Wang, G.D. and Dixon, R.A. (2009) Heterodimeric geranyl(geranyl)diphosphate synthase from hop (*Humulus lupulus*) and the evolution of monoterpene biosynthesis. *Proc. Natl Acad. Sci. USA*, **106**, 9914–9919.

Wang, K.C. and Ohnuma, S. (2000) Isoprenyl diphosphate synthases. *Biochim. Biophys. Acta*, **1529**, 33–48.

Wang, Y., Dreyfuss, M., Ponelle, M., Oberer, L. and Riezman, H. (1998) A glycosylphosphatidylinositol-anchoring inhibitor with an unusual tetracarbocyclic sesterterpene skeleton from the fungus *Codinaea simplex*. *Tetrahedron*, **54**, 6415–6426.

Wang, Q.X., Yang, J.L., Qi, Q.Y. *et al.* (2013) 3–Anhydro-6–hydroxy-ophiobolin A, a new sesterterpene inhibiting the growth of methicillin-resistant *Staphylococcus aureus* and inducing the cell death by apoptosis on K562, from the phytopathogenic fungus *Bipolaris oryzae*. *Bioorg. Med. Chem. Lett.*, **23**, 3547–3550.

Wessjohann, L.A and Dessoy, M.A. (2004) Silylierte Oligophosphate, Phosphate und Phosphite und Verfahren zu deren Herstellung und Alkylierung. Patent DE102004033306A1 [WWW document]. URL http://www.google.com/patents/DE102004033306A1?cl=de [accessed on 4 November 2015].

Wessjohann, L.A. and Dessoy, M.A. (2014) An efficient method for the preparation of silyl esters of diphosphoric, phosphoric, and phosphorous acid. *Polyhedron*, **70**, 133–137.

Zhu, X.F., Suzuki, K., Okada, K., Tanaka, K., Nakagawa, T., Kawamukai, M. and Matsuda, H. (1997a) Cloning and functional expression of a novel geranylgeranyl pyrophosphate synthase gene from *Arabidopsis thaliana* in *Escherichia coli*. *Plant Cell Physiol.*, **38**, 357–361.

Zhu, X.F., Suzuki, K., Saito, T., Okada, K., Tanaka, K., Nakagawa, T., Matsuda, H. and Kawamukai, M. (1997b) Geranylgeranyl pyrophosphate synthase encoded by the newly isolated gene GGPS6 from *Arabidopsis thaliana* is localized in mitochondria. *Plant Mol. Biol.*, **35**, 331–341.

